

EfficientDreamer: High-Fidelity and Robust 3D Creation via Orthogonal-view Diffusion Prior

Minda Zhao¹, Chaoyi Zhao¹, Xinyue Liang¹, Lincheng Li^{1*}, Zeng Zhao¹, Zhipeng Hu¹
Changjie Fan¹, Xin Yu²

¹NetEase Fuxi AI Lab, ² University of Queensland

{zhaominda01, zhaochaoyi, liangxinyue03, lilincheng, hzzhaozeng, zphu, fanchangjie}@corp.netease.com,
xin.yu@uq.edu.au

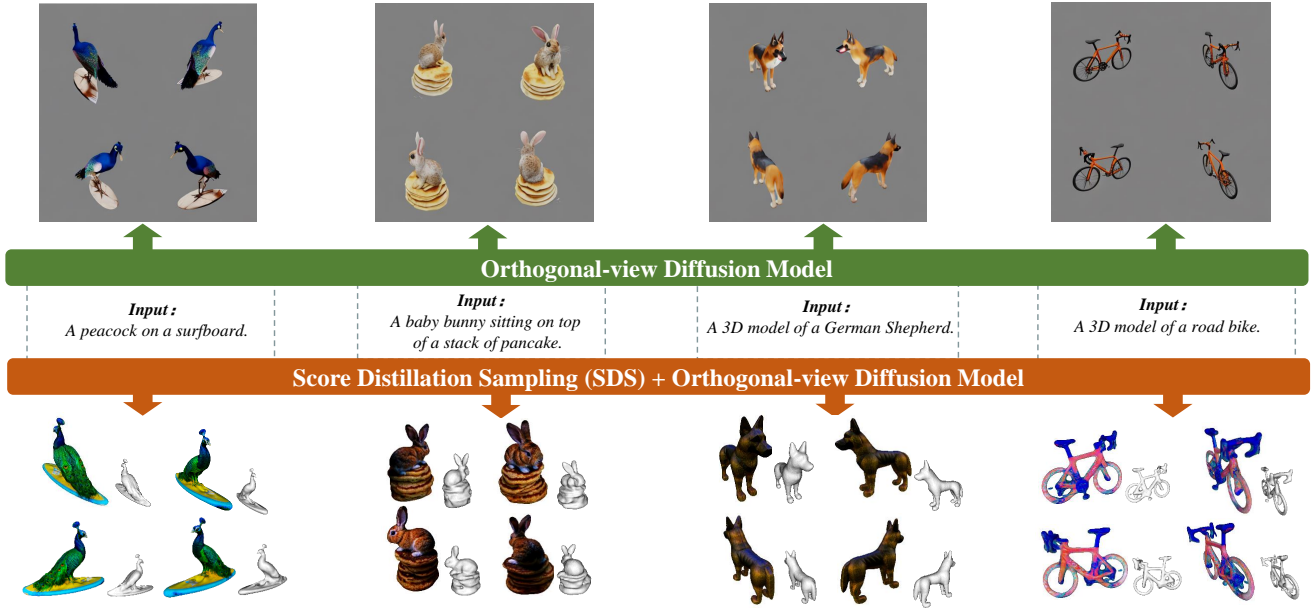


Figure 1. *EfficientDreamer* can create high-fidelity 3D contents with given text prompts. It relies on the newly introduced orthogonal-view diffusion model which can generate 3D consistent images of an identical scene from orthogonal viewpoints.

Abstract

While the image diffusion model has made significant strides in text-driven 3D content creation, it often falls short in accurately capturing the intended meaning of the text prompt, particularly with respect to direction information. This shortcoming gives rise to the Janus problem, where multi-faced 3D models are produced with the guidance of such diffusion models. In this paper, we present a robust pipeline for generating high-fidelity 3D content with orthogonal-view image guidance. Specifically, we introduce a novel 2D diffusion model that generates an image

consisting of four orthogonal-view sub-images for the given text prompt. The 3D content is then created with this diffusion model, which enhances 3D consistency and provides strong structured semantic priors. This addresses the infamous Janus problem and significantly promotes generation efficiency. Additionally, we employ a progressive 3D synthesis strategy that results in substantial improvement in the quality of the created 3D contents. Both quantitative and qualitative evaluations show that our method demonstrates a significant improvement over previous text-to-3D techniques.

*Corresponding author

1. Introduction

The field of generating photorealistic 2D images from simple text prompts is rapidly growing, and recent advancements owe much to the use of diffusion models. This has resulted in the development of models that can generate images of exceptional quality [24–26]. In contrast, generating high-quality 3D content from text prompts is a much more challenging field, given that the output space is significantly larger and 3D consistency is required. Additionally, there is a lack of large amounts of training data pairs for text and 3D models, which further complicates the development of effective models in this domain.

Early methods [9, 13, 20] explore zero-shot text-guided 3D content creation utilizing the guidance from CLIP [23]. These approaches optimize the underlying 3D representations (NeRFs and meshes), such that all 2D renderings reach high text-image alignments scores. However, they tend to generate poor 3D shapes with unsatisfactory geometry as well as appearance. To overcome such limitations, DreamFusion [22] showcased impressive capability in text-to-3D synthesis by utilizing a powerful pre-trained text-to-image diffusion model [25] as a strong image prior. With novel Score Distillation Sampling (SDS) gradients together with view-dependent prompts, they train a NeRF to represent 3D models. Some follow-up works focus on further improving the quality of the generated content, such as TextMesh [31], Magic3D [15], and ProlificDreamer [34].

While previous methods have demonstrated impressive results, a significant drawback is the Janus problem, which remains a major challenge to overcome. According to recent studies [17], the primary cause of the Janus problem lies in the inability of pre-trained 2D diffusion models to accurately interpret the view instructions specified in the text prompts. The quality of created 3D contents heavily depends on the random guidance of the diffusion model at early steps, which makes such a procedure unstable.

To cope with these weaknesses, we proposed a new method called *EfficientDreamer*, a novel framework designed for high-quality and robust 3D creation via a novel diffusion prior. With access to unprecedented amounts of training data (over 5 billion images), modern generative models have achieved state-of-the-art performance, and diffusion models have emerged as the leading representation of natural image distribution. These models can capture a vast range of objects from multiple viewpoints, providing extensive support for image-generation tasks. We demonstrate that we are able to optimize the data distribution and generate identical content from different viewpoints while keeping high 3D consistency. To this end, we train a new image diffusion model with a large-scale open-source 3D object dataset. Given a text prompt, this diffusion model can output a composite image, which comprises four sub-images from orthogonal views. These sub-images may come from

arbitrary viewpoints but keep the relationship of clockwise rotation. Our belief is that a set of four orthogonal-view images can effectively convey most of the object’s semantic information and facilitate precise view instructions.

With this novel image diffusion model, we can create high-fidelity and robust 3D content through SDS loss back-propagation. In each training step, we differentially render four images from orthogonal viewpoints, and these four images are tiled on a 2×2 grid as a composite image. Then the images are employed to calculate the SDS loss and further optimized the 3D representation. In this way, we obtain 3D consistency between different 2D views. Our approach not only enables the efficient generation of 3D models but also eliminates the Janus problem suffered by most existing methods.

While the novel diffusion model provides crucial structured guidance for 3D creation, strict geometry consistency can not be guaranteed. Relying solely on such orthogonal-view diffusion prior may result in local artifacts, such as holes in the reconstructed 3D content. To solve this problem, we also introduce the original stable diffusion model as 2D prior. We further introduce a progressive 3D synthesis strategy to balance the guidance of the orthogonal-view diffusion prior and pre-trained 2D diffusion prior. At an early stage, rough 3D geometry generation is mainly concerned and large-weight orthogonal-view diffusion prior leads to the efficient geometry representation, which alleviate Janus problem as well. Once the initial 3D shape is complete enough, we gradually reduce the weight of orthogonal-view diffusion prior and increase the original 2D diffusion guidance. The original 2D diffusion prior can facilitate local texture detail generation and geometry smoothness.

To generate high-quality 3D mesh representations with photorealistic texture from text prompts, we introduce a two-stage coarse-to-fine optimization process. In the coarse stage, we utilize NeuS (Neural Implicit Surfaces by Volume Rendering) representation [33] due to its state-of-the-art performance and simple design. In the second stage, we employ Deep Marching Tetrahedra (DMTet) [29] to refine the geometry and texture separately. In the first stage, we leverage the progressive 3D synthesis strategy to guide the 3D creation, while adopting the original 2D diffusion prior for the second-stage optimization.

The overall contributions are as follows:

- We propose *EfficientDreamer*, a new method for high-fidelity and robust 3D creation using orthogonal-view diffusion prior. This method addresses the infamous Janus problem and significantly stabilizes the generation process.
- We introduce a novel image diffusion model, which can generate a composite image consisting of four sub-image from orthogonal viewpoints. These four

orthogonal-view images can cover most of the semantic information of identity objects, and can provide specific geometry instructions.

- We propose a novel text-driven 3D creation pipeline based on improved Score Distillation Sampling (SDS) loss. A progressive 3D synthesis strategy is employed to combine the original 2D diffusion prior and newly-trained orthogonal-view diffusion prior, which ensures the high quality of generated 3D contents.

2. Related work

2.1. 3D Reconstruction with Neural Fields

Traditional Multi-View Stereo methods reconstruct 3D point clouds from the predicted depth maps [6, 27, 35, 43]. Benefiting from deep learning, supervised MVS methods have also become popular [7, 32, 36–38]. These methods show impressive performance on multiple benchmarks [10, 11], but they have to be trained on specific datasets [10, 39]. These systems often fail in less constrained scenarios and cannot be integrated easily into other learning-based systems. On the other hand, in recent times, there have been significant advancements in neural fields that have demonstrated remarkable results across various tasks. As a famous neural volume rendering method, NeRF [5, 19, 21, 41] combines classical volumetric rendering with implicit function to render high-quality 2D images. However, directly extracting a mesh from a NeRF representation is non-trivial [30]. Recent works have focused on improving the geometric network while establishing connections between density-based and surface-based representations. VolSDF [40] models the volume density as Laplace Cumulative Distribution Function applied to an SDF representation. Similar to VolSDF, NeuS [33] transforms the SDF field to the accumulated transmittance for volume rendering with the Logistic Cumulative Distribution Function and it is pointed that the rendered weight should reach the maximum at the first intersection point from outside to inside. To this end, we adopt the NeuS representation for the convenience of mesh extraction.

2.2. Text-to-image Generation

In recent years, with the availability of extremely large datasets of image-text pairs [28], significant progress has been made in text-to-image generation with diffusion models. A typical method is the Stable Diffusion model, which samples from a lower-resolution latent space and decodes latent into high-resolution images. [25]. Such sampling operation in the latent greatly improves the efficiency of image generation. Another kind of method utilizes a cascade of super-resolution models. [2, 26]. These methods first generate a low-resolution image from a given text prompt and

then enlarge the images with several super-resolution models. Recent works design special neural network structures to control diffusion models by adding extra conditions [42], it can learn task-specific input conditions and produce customized images. Due to the strong generative ability of pre-trained diffusion models, they are convenient to enable text-to-3D mesh synthesis.

2.3. Text-to-3D Generation

In recent years, text-to-3D has received significant attention due to the desire to create high-quality 3D content from simple semantics, such as text prompts. Early works attempt to use a CLIP objective to supervise the generation. CLIPMesh [20] deforms a 3D sphere using a CLIP loss to obtain a 3D mesh that fits the input prompt. Text2Mesh [18] stylizes a 3D mesh by predicting color and local geometric details which conform to a target text prompt. Dreamfield [9] optimizes a Neural Radiance Field from many camera views so that rendered images score highly with a target caption according to a pre-trained CLIP model. However, these methods tend to generate poor 3D shapes with unsatisfactory geometry as well as appearance. To overcome such limitations, DreamFusion [22] employs text-to-3D synthesis by utilizing a powerful pre-trained text-to-image diffusion model as a strong image prior. They optimize NeRF with their proposed Score Distillation Sampling (SDS) loss. Magic3D [15] extends such a method to a two-stage coarse-to-fine process, which utilized DM Tet for mesh representation. Fantasia3D [3] disentangles geometry and appearance into a two-stage optimization and introduces the spatially varying bidirectional reflectance distribution function (BRDF) into the text-to-3D task. TextMesh [31] replaces NeRF with VolSDF for more accurate mesh expression. It proposes a novel multi-view consistent and mesh-conditioned re-texturing, enabling the generation of a photorealistic 3D mesh model. More recently, ProlificDreamer [34] proposes *variational score distillation* (VSD), a principled particle-based variational framework to promote the quality of created 3D models.

3. Methodology

Given a text prompt y , our goal is to create high-quality 3D mesh representations with photorealistic texture. We first introduce a new orthogonal-view diffusion model which can generate composite images containing four orthogonal-view sub-images, which is denoted as ϕ_{ov} . Then we perform text-to-3D with a progressive 3D synthesis strategy, which combines the orthogonal-view diffusion model and pre-trained diffusion model (i.e., ϕ_{pre}) to promote the quality of the created 3D contents.

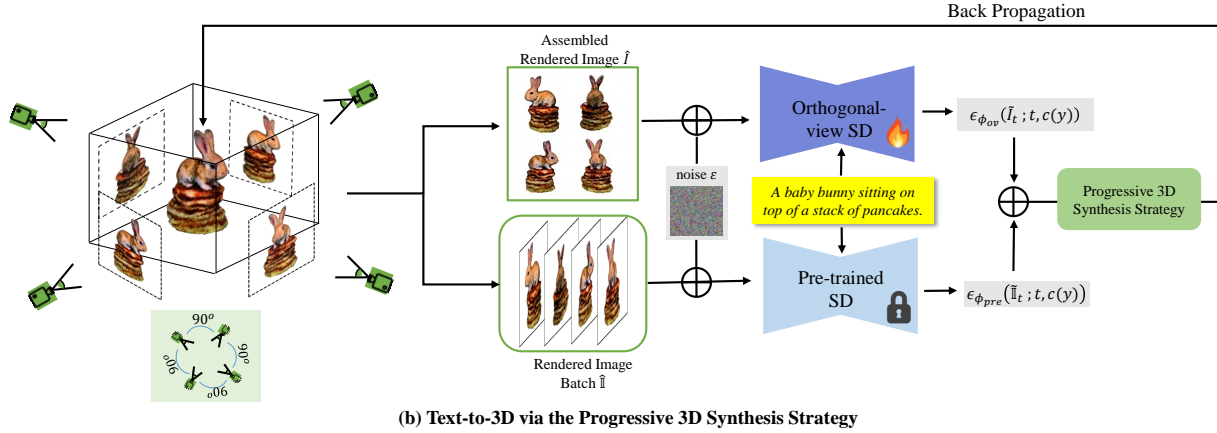
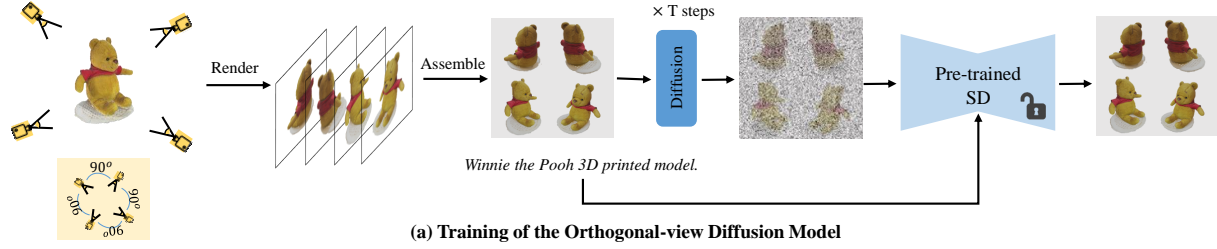


Figure 2. The overview of EffcientDreamer. We first train an orthogonal-view diffusion model by rendering images of the Objaverse dataset. Then we optimize 3D scene representation, which is guided by the newly-introduced orthogonal-view diffusion model and the pre-trained text-to-image diffusion model. The progressive 3D synthesis strategy is utilized to achieve high-fidelity and robust 3D creation.

3.1. 3D Scene Representation

Coarse stage While NeRF achieves impressive view synthesis results, the density-based representation is not well-suited for extracting a 3D geometry and obtaining a mesh [40]. In this paper, we adopt NeuS as the 3D scene representation in the coarse stage.

Given a point \mathbf{p} and a unit viewing direction \mathbf{v} , the ray emitted from the camera center \mathbf{o} at the viewing direction \mathbf{v} is denoted as $\{\mathbf{p}(t) = \mathbf{o} + t\mathbf{v} | t \geq 0\}$. The volumetric rendering of the radiance field can be represented as

$$T(t) = \exp(-\int_0^t \sigma(u) du), \quad w(t) = T(t)\sigma(t) \quad (1)$$

$$\hat{C} = \int_0^{+\infty} w(t)c(\mathbf{p}(t), \mathbf{v})dt, \quad \hat{t} = \int_0^{+\infty} w(t)t dt$$

where $\sigma(t)$ is the volume density, $T(t)$ is the accumulated transmittance along the ray, \hat{C} and \hat{t} denote the rendered color and depth along the ray, respectively. $w(t)$ can be regarded as the weight function along the ray, which is formulated as

$$w(\mathbf{p}(t)) = \max \left(-f'(\mathbf{p}(t))\Psi'_\beta(f(\mathbf{p}(t))), 0 \right), \quad (2)$$

where the Signed Distance Function $f(\mathbf{p})$ means the minimal signed distance between a point \mathbf{p} and the surface.

Fine stage During the refinement stage of our optimization process, we use textured 3D meshes as the scene representation, with which rendering textured meshes with differentiable rasterization can be performed efficiently at very high resolutions.

We represent the 3D shape with a deformable tetrahedral grid (V_T, T) , where V_T is the vertices in the grid T . Each vertex $v_i \in V_T$ contains a signed distance field (SDF) value and deformation of the vertex from its initial canonical coordinate. The surface mesh can be extracted from the SDF value while the texture can be calculated with the neural color field.

3.2. Orthogonal-view Diffusion Model

Our objective is to use a fine-tuned diffusion model to generate a composite image in response to a given text prompt y . The composite image is expected to contain four sub-images from orthogonal point views, which are tiled on a 2×2 grid.

Since common text-to-image diffusion models are trained with large-scale text-image pairs, they own the ability to describe objects from many viewpoints. However, they lack explicitly aligning the correspondences of an identical object between viewpoints. Moreover, they tend to

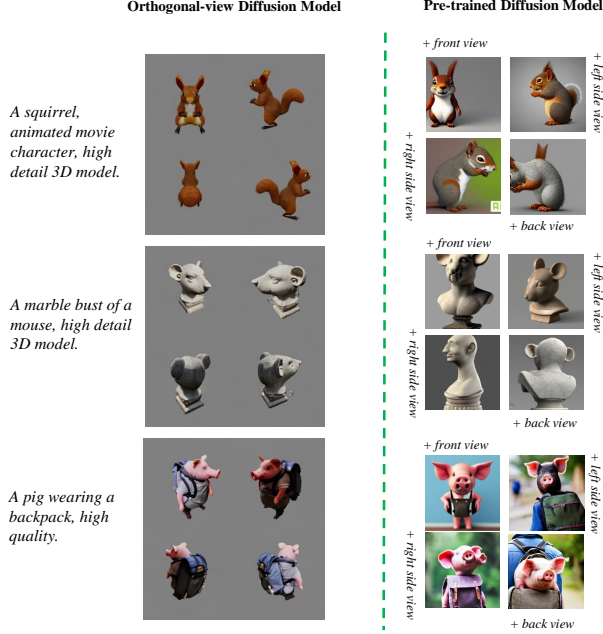


Figure 3. Comparison between the orthogonal-view diffusion model and pre-trained diffusion model. The composite images generated by our orthogonal-view diffusion model are shown on the left. Each image contains four sub-images from four orthogonal viewpoints. The outputs of the pre-trained diffusion model are shown on the right.

generate images of objects in canonical poses. Thus, it is crucial to introduce a novel diffusion model which can generate exhibitions of an identical object from significant views while keeping the 3D consistency among them. In this paper, we claim the showcases from four orthogonal views are appropriate and can cover most semantic instructions of the object.

To obtain such a specific image diffusion model, we use the recently released Objaverse [4] dataset for fine-tuning the common-used diffusion model, i.e., Stable Diffusion model. This dataset contains 800K+ 3D models created by 100K+ artists. The descriptions for each 3D model can be found in Cap3D [16] dataset, which is processed with BLIP2 [14] and GPT4. We first filter some improper 3D models, like complex scene representation, textureless 3D models, and point clouds, and approximately 420K high-quality 3D models are left. We normalize all assets into a unit cube $[-0.5, 0.5]^3$ and radius (distance away from the center) is set at 1.8. For each 3D model, we uniformly render 12 images in the range of azimuth angle $\xi_{cam} \in (0^\circ, 360^\circ)$ and elevation angle list $\delta_{cam} = [0^\circ, 15^\circ, 30^\circ, 45^\circ]$. Thus, for each 3D asset, we render 48 RGBA images in 512×512 resolution in total while its corresponding text prompt is denoted as y . We use the Sta-

ble Diffusion 2.1 as the original latent diffusion architecture with an encoder \mathcal{E} , a denoiser U-Net ϵ_θ , and a decoder \mathcal{D} . We utilize \mathcal{E} and \mathcal{D} with pre-trained weight and only fine-tune ϵ_θ for generating composite images from orthogonal views. For each training step, we first sample an elevation angle from the elevation angle list and then select four render images in this elevation angle, the rendered images are required to be 90 degrees apart from each other in azimuth angle. Then these four images are tiled on a 2×2 grid in a clockwise rotation. To match the diffusion model, we resize this composite image into 512×512 resolution, which is denoted as x . Let $c(y)$ be the embedding of y and diffusion time step $t \sim [1, 1000]$, we then solve for the following objective to fine-tune the model:

$$\min_{\theta} \mathbb{E}_{z \sim \mathcal{E}(x), t, \epsilon \sim \mathcal{N}(0, 1)} \|\epsilon - \epsilon_\theta(z_t, t, c(y))\|^2. \quad (3)$$

We find the trained diffusion model can learn a generic mechanism to explicitly align the correspondence of an identical object from different viewpoints, even for objects never appear in the training dataset. The comparison between the orthogonal-view diffusion model and the pre-trained diffusion model is shown in Fig. 3.

3.3. Text-to-3D via the Progressive 3D Synthesis Strategy

Once the orthogonal-view diffusion model is trained, we can generate our initial 3D model by training a neural distance field using the score distillation sampling strategy. The scene is represented as a differential render $g(\psi)$, where ψ denotes the learnable parameters. Given a randomly sampled camera pose with azimuth angle ξ_{cam} , elevation angle δ_{cam} and radius r , we fix δ_{cam} and r and sample four camera poses by extending ξ_{cam} to $[\xi_{cam}, \xi_{cam} + 90^\circ, \xi_{cam} + 180^\circ, \xi_{cam} + 270^\circ]$. Then we render images with these camera poses, which are denoted as I_0, I_1, I_2, I_3 . We also tiled them on a 2×2 grid in a clockwise rotation and resize the composite image into 512×512 resolution, which is denoted as \hat{I} . Then we sample random normal noise according to time step t and add it to \hat{I} . The noisy images \tilde{I}_t , together with text embedding $c(y)$ are fed to our orthogonal-view diffusion model ϕ_{ov} , which attempts to predict the noise ϵ . The denoiser U-Net of ϕ_{ov} is denoted as $\epsilon_{\phi_{ov}}$ and the score function of noise estimation is denoted as $\epsilon_{\phi_{ov}}(\tilde{I}_t; t, c(y))$. This score function guides the direction of the gradient for updating the scene parameters, and the gradient is calculated by Score Distillation Sampling (SDS):

$$\nabla_{\psi} \mathcal{L}_{SDS}^{ov} = \mathbb{E}_{t, \epsilon} [\omega(t) (\epsilon_{\phi_{ov}}(\tilde{I}_t; t, c(y)) - \epsilon) \frac{\partial \hat{I}}{\partial \psi}], \quad (4)$$

where $\omega(t)$ denotes a weighting function.

Motivated by [8] and to increase the stability of the training procedure, we decrease time step t as training executes, which means the degree of added noise declines gradually. Since our training procedure supervises the 3D creation from four orthogonal views at each time, the neural distance field can receive semantic structure guidance from different viewpoints and thus eliminates the possibility of creating multi-face problems in principle.

While training 3D scene representation via the orthogonal-view model prior can alleviate the Janus problem, the quality of generated 3D models may decline, such as unexpected holes in the surface of generated 3D models. We find the 3D consistency among the sub-images in the composite image from the orthogonal-view diffusion model can be less rigid. Due to the 2D attribute of the image diffusion model, it is impractical to achieve 3D geometry consistent over different views.

To resolve such a problem, we incorporate the proposed orthogonal-view model and original text-to-image diffusion model to guide the 3D model generation with a progressive strategy. Let $\epsilon_{\phi_{pre}}$ denote the denoiser U-Net of the pre-trained diffusion model, and rearrange the original rendered images I_0, I_1, I_2, I_3 as an image batch $\hat{\mathbb{I}}$. $\tilde{\mathbb{I}}_t$ denotes the noisy result of $\hat{\mathbb{I}}$. The corresponding SDS loss is formulated as:

$$\nabla_{\psi} \mathcal{L}_{SDS}^{pre} = \mathbb{E}_{t, \epsilon} [\omega(t) (\epsilon_{\phi_{pre}}(\tilde{\mathbb{I}}_t; t, c(y)) - \epsilon) \frac{\partial \hat{\mathbb{I}}}{\partial \psi}]. \quad (5)$$

We propose a new prior loss for the novel view supervision to combine both two priors:

$$\nabla_{\psi} \mathcal{L}_{SDS} = (1 - (\frac{l}{L})^{\lambda}) \nabla_{\psi} \mathcal{L}_{SDS}^{ov} + (\frac{l}{L})^{\lambda} \nabla_{\psi} \mathcal{L}_{SDS}^{pre}, \quad (6)$$

where l is the current iteration while L is the total iterations. λ is a hyperparameter to determine the strength of two diffusion priors, which is set as 1 in our experiments.

4. Experiments

In this section, we present comprehensive experiments to evaluate the efficacy of our proposed method for text-to-3D content creation. We first show visual results of coarse and fine stages in our framework in 4.1, and then compare the capacity of 3D creation with some state-of-the-art methods, containing DreamFusion [22], Magic3D [15], TextMesh [31]. Visual results are shown in 4.2. Then we compare our method with another method which can alleviate Janus problem, i.e., Perp-Neg [1] in 4.3. In 4.4, we conduct a user study for quantifying the subjective quality. Finally, an ablation study is shown in 4.5 to analyze the 3D consistency of our introduced orthogonal-view diffusion and the effect of the progressive 3D synthesis strategy.

4.1. Coarse-to-fine Two-stage Optimization Results

We show the 3D contents generated through the coarse and fine stages in our optimization procedure in Fig. 4. In the coarse stage, we can obtain the rough shape and texture representation for the given text prompts. With the guidance of the orthogonal-view diffusion model, the results become more semantically reasonable. The fine stage initializes the mesh representation with the results of the coarse stage, and it optimizes the geometry and texture through differentiable rasterization. We can then generate much higher-quality 3D models.

4.2. Comparison with State-of-the-art

We present comprehensive experiments to evaluate the efficacy of our proposed method for text-to-3D content creation. The compared methods include three crucial Text-to-3D methods, i.e., DreamFusion [22], Magic3D [15] and TextMesh [31]. All these methods are implemented with a unified framework for 3D content creation¹. As DreamFusion and TextMesh generate 3D contents with volume rendering of 64×64 resolution, the generated 3D models may suffer from over-smoothness and lack of details. However, Magic3D can generate much higher quality 3D shapes on both geometry and texture. Since our method also utilizes a coarse-to-fine two-stage optimization, we can create high-quality 3D mesh models. Moreover, all these compared methods may be confronted with Janus problem as they guide the 3D creation with open-source pre-trained diffusion prior, which does not perform valid 3D consistency constraint. Our method can resolve the multi-face problem with our newly-introduced orthogonal-view diffusion prior.

We also evaluate our method using the CLIP Score [23] and FID [12]. CLIP Score metric measures how well images rendered from the generated geometry correlate with the provided input text prompt while FID evaluates the quality and photorealistic appearance of the generated shapes. We use the ImageNet 2012 validation set as reference images and render four images with fixed camera poses for each 3D model. The results are depicted in Table 1, which demonstrates that our methods achieve better performance than the state-of-the-arts.

4.3. Comparison with Perp-Neg

Here we also compare our method with another method which is proposed to alleviate Janus problem. i.e., Perp-Neg [1]. We employ this method to DreamFusion and compare it with our method. The results are depicted in Fig. 6. The Perp-Neg can alleviate Janus problem in some cases. For example, it can generate 3D models with only one head and face. However, the results may contain unreasonable details, like three eyes, five legs, and so on. Since our

¹<https://github.com/threestudio-project/threestudio>

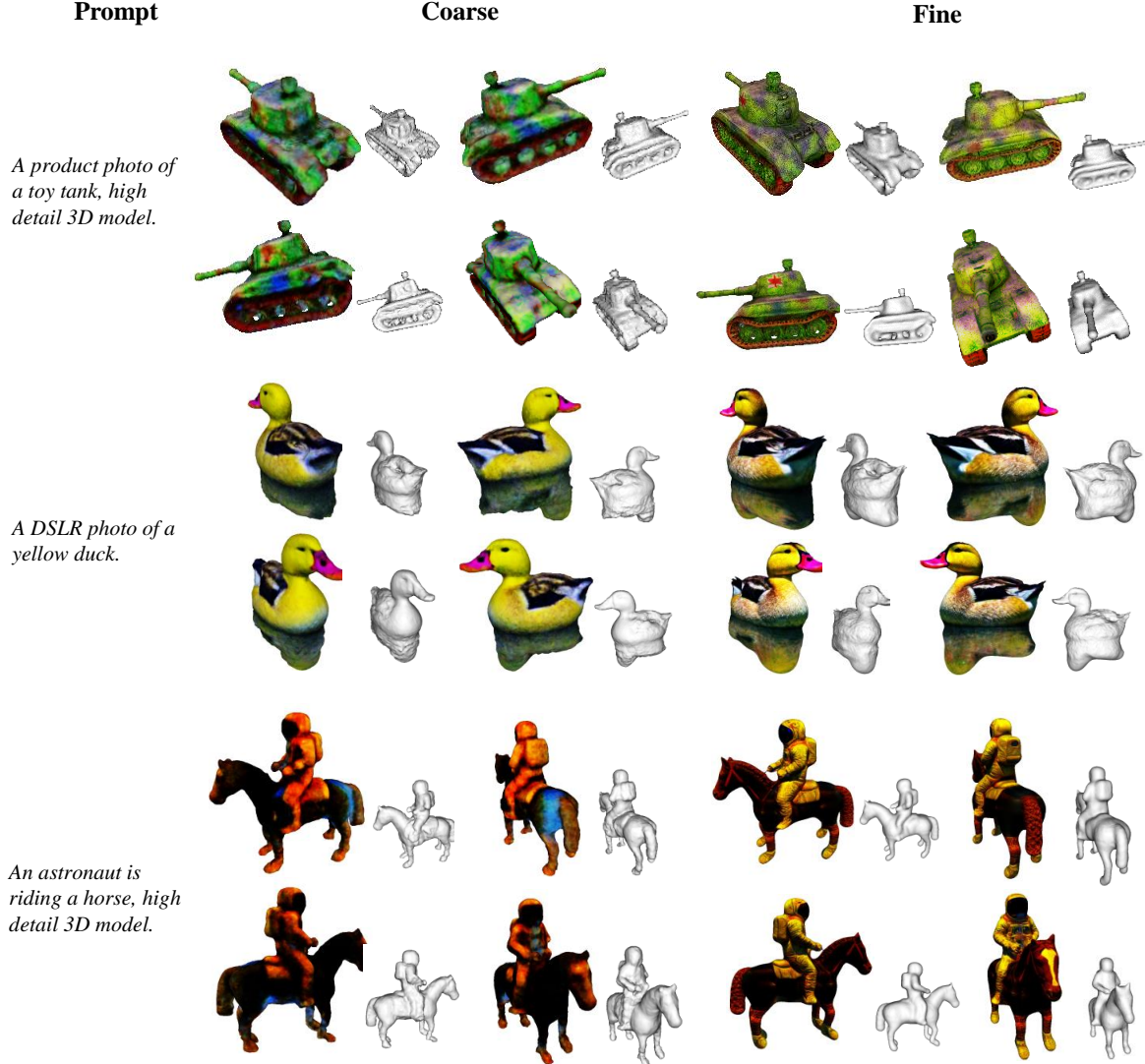


Figure 4. Coarse-to-fine two-stage optimization results. In the coarse stage, we get semantically reasonable 3D scene representation. In the fine stage, we improve the visual quality of generated 3D assets

Table 1. Comparison with state-of-the-arts. Comparing our method against the state-of-the-arts using CLIP score and FID. The metrics are computed on 22 prompts. ↓ indicates the lower the better, and ↑ indicates the higher the better.

Methods	CLIP Score ↑	FID ↓
DreamFusion [22]	28.40	374.44
Magic3D [15]	29.15	310.57
TextMesh [31]	27.65	305.77
Ours	30.33	284.98

method guides the 3D creation with orthogonal views at the same time, we can avoid such problems.

4.4. User Study

We conduct a user study with Fuxi Youling Crowdsourcing² for quantifying the subjective quality. Concretely, the ablation is evaluated on 22 prompts. At each evaluation time, the participants are shown the created 3D models by DreamFusion [22], Magic3D [15], TextMesh [31] and our method, and asked to rate them from 1 to 4. In total, we have collected 1100 responses contributed by 50 participants. The average rating scores for different methods are depicted in Table 2, where a higher score means a more realistic and detailed result. Additionally, we calculate the the users’ preference ratio for results of each method with

²<https://fuxi.163.com/solution/data>



Figure 5. Comparison with other text-to-3D methods. For each 3D model, we render it from two views with a textureless rendering for each view. Our method creates more high-fidelity 3D models without the Janus problem.



Figure 6. Comparison between the Perp-Neg and our methods. We solved the Janus problem more thoroughly.

Table 2. Results of our user study, conducted with 50 participants. Each participant was shown meshes generated by different methods. The rating score represents the average rating results for different methods, while the preference denotes the users’ preference ratio for results of each method with higher quality. A total of 22 prompts are utilized.

Methods	Rating Score \uparrow	Preference(%) \uparrow
DreamFusion [22]	2.09	4.55
Magic3D [15]	2.44	6.27
TextMesh [31]	1.73	4.91
Ours	3.74	84.27

higher quality. 84.27% of the users consider our results with higher quality than all competitors. The above results further verify that our method generates visually high-fidelity 3D models from the perspective of users.

4.5. Ablation Study

We introduce a progressive 3D synthesis strategy in the coarse stage in our framework. Here we provide analysis and experiments to show its effectiveness.

Given several text prompts, we employ 3D creation with different diffusion model guidances at the coarse stage with the rendering of 64x64 resolution. We optimize the 3D scene representation with NeuS and then extract meshes with MarchingTet. The corresponding results are shown in Fig. 7. The first four columns demonstrate the results with our progressive 3D synthesis strategy, which means $\lambda = 1$. We get complete and smooth meshes and eliminate the possible Janus problem. The next four columns demonstrate the result guided with the pure orthogonal-view diffusion model, which is equivalent to $\lambda = 0$. While such an op-

eration can provide comprehensive structure constraints for 3D generation and restrain multi-face issues, the rough 3D consistency between different views in the generated sub-images may impede convergence during the late optimization period. Thus we can see apparent holes and unreasonable roughness. The last four columns show the results generated with pure original pre-trained diffusion model, which is equivalent to $\lambda = \infty$. Obvious Janus problems can be found for the first two prompts. As for the creation of a cottage, we get similar shapes from different viewpoints. However, the results with the progressive 3D synthesis strategy are more reasonable.

5. Conclusion

In this paper, we present *EfficientDreamer*, a novel high-fidelity and robust 3D creation method via orthogonal-view diffusion prior. In the core, we introduce a novel diffusion model which can generate a composite image consisting of sub-images from four orthogonal viewpoints. Given a text prompt, these showcases of an identical object from crucial views can provide a more adequate semantic representation. Then we can improve the text-to-3D generation framework with this novel orthogonal-view diffusion model. We also employ a progressive strategy that adaptively incorporates the orthogonal-view diffusion prior and the original pre-trained diffusion prior. Our method can address the infamous Janus problem while keeping the high fidelity of 3D creation.

References

- [1] Mohammadreza Armandpour, Huangjie Zheng, Ali Sadeghian, Amir Sadeghian, and Mingyuan Zhou. Re-imagine the negative prompt algorithm: Transform 2d

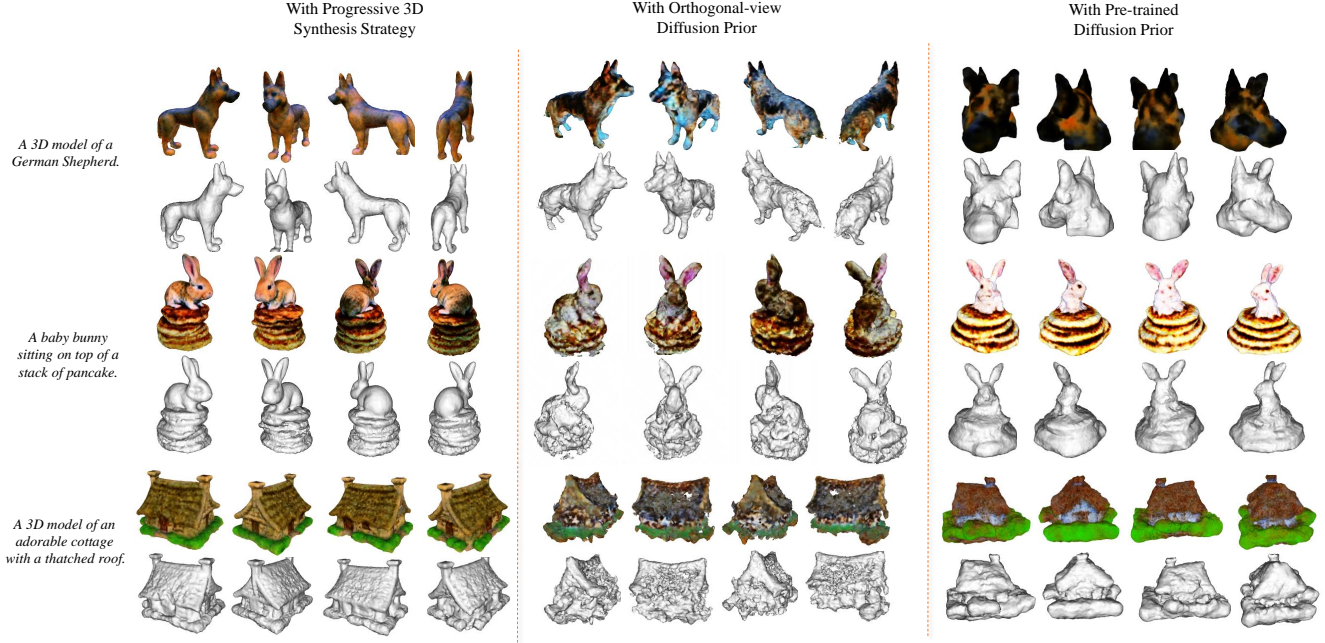


Figure 7. Ablation study of the progressive 3D synthesis strategy.

- diffusion into 3d, alleviate janus problem and beyond. *arXiv preprint arXiv:2304.04968*, 2023. 6
- [2] Yogesh Balaji, Seungjun Nah, Xun Huang, Arash Vahdat, Jiaming Song, Karsten Kreis, Miika Aittala, Timo Aila, Samuli Laine, Bryan Catanzaro, et al. ediffi: Text-to-image diffusion models with an ensemble of expert denoisers. *arXiv preprint arXiv:2211.01324*, 2022. 3
- [3] Rui Chen, Yongwei Chen, Ningxin Jiao, and Kui Jia. Fantasia3d: Disentangling geometry and appearance for high-quality text-to-3d content creation. *arXiv preprint arXiv:2303.13873*, 2023. 3
- [4] Matt Deitke, Dustin Schwenk, Jordi Salvador, Luca Weihs, Oscar Michel, Eli VanderBilt, Ludwig Schmidt, Kiana Ehsani, Aniruddha Kembhavi, and Ali Farhadi. Objaverse: A universe of annotated 3d objects. In *Proceedings of the IEEE/CVF Conference on Computer Vision and Pattern Recognition*, pages 13142–13153, 2023. 5
- [5] Sara Fridovich-Keil, Alex Yu, Matthew Tancik, Qinhong Chen, Benjamin Recht, and Angjoo Kanazawa. Plenoxels: Radiance fields without neural networks. In *Proceedings of the IEEE/CVF Conference on Computer Vision and Pattern Recognition*, pages 5501–5510, 2022. 3
- [6] Silvano Galliani, Katrin Lasinger, and Konrad Schindler. Massively parallel multiview stereopsis by surface normal diffusion. In *Proceedings of the IEEE International Conference on Computer Vision*, pages 873–881, 2015. 3
- [7] Xiaodong Gu, Zhiwen Fan, Siyu Zhu, Zuozhuo Dai, Feitong Tan, and Ping Tan. Cascade cost volume for high-resolution multi-view stereo and stereo matching. In *Proceedings of the IEEE/CVF conference on computer vision and pattern recognition*, pages 2495–2504, 2020. 3
- [8] Yukun Huang, Jianan Wang, Yukai Shi, Xianbiao Qi, Zheng-Jun Zha, and Lei Zhang. Dreamtime: An improved optimization strategy for text-to-3d content creation. *arXiv preprint arXiv:2306.12422*, 2023. 6
- [9] Ajay Jain, Ben Mildenhall, Jonathan T Barron, Pieter Abbeel, and Ben Poole. Zero-shot text-guided object generation with dream fields. In *Proceedings of the IEEE/CVF Conference on Computer Vision and Pattern Recognition*, pages 867–876, 2022. 2, 3
- [10] Rasmus Jensen, Anders Dahl, George Vogiatzis, Engin Tola, and Henrik Aanæs. Large scale multi-view stereopsis evaluation. In *Proceedings of the IEEE conference on computer vision and pattern recognition*, pages 406–413, 2014. 3
- [11] Arno Knapitsch, Jaesik Park, Qian-Yi Zhou, and Vladlen Koltun. Tanks and temples: Benchmarking large-scale scene reconstruction. *ACM Transactions on Graphics (ToG)*, 36(4):1–13, 2017. 3
- [12] Tuomas Kynkäänniemi, Tero Karras, Miika Aittala, Timo Aila, and Jaakko Lehtinen. The role of imagenet classes in fr\`echet inception distance. *arXiv preprint arXiv:2203.06026*, 2022. 6
- [13] Han-Hung Lee and Angel X Chang. Understanding pure clip guidance for voxel grid nerf models. *arXiv preprint arXiv:2209.15172*, 2022. 2
- [14] Junnan Li, Dongxu Li, Silvio Savarese, and Steven Hoi. Blip-2: Bootstrapping language-image pre-training with frozen image encoders and large language models. *arXiv preprint arXiv:2301.12597*, 2023. 5
- [15] Chen-Hsuan Lin, Jun Gao, Luming Tang, Towaki Takikawa, Xiaohui Zeng, Xun Huang, Karsten Kreis, Sanja Fidler,

- Ming-Yu Liu, and Tsung-Yi Lin. Magic3d: High-resolution text-to-3d content creation. In *Proceedings of the IEEE/CVF Conference on Computer Vision and Pattern Recognition*, pages 300–309, 2023. 2, 3, 6, 7, 9
- [16] Tiange Luo, Chris Rockwell, Honglak Lee, and Justin Johnson. Scalable 3d captioning with pretrained models. *arXiv preprint arXiv:2306.07279*, 2023. 5
- [17] Gal Metzer, Elad Richardson, Or Patashnik, Raja Giryes, and Daniel Cohen-Or. Latent-nerf for shape-guided generation of 3d shapes and textures. In *Proceedings of the IEEE/CVF Conference on Computer Vision and Pattern Recognition*, pages 12663–12673, 2023. 2
- [18] Oscar Michel, Roi Bar-On, Richard Liu, Sagie Benaim, and Rana Hanocka. Text2mesh: Text-driven neural stylization for meshes. In *Proceedings of the IEEE/CVF Conference on Computer Vision and Pattern Recognition*, pages 13492–13502, 2022. 3
- [19] Ben Mildenhall, Pratul P Srinivasan, Matthew Tancik, Jonathan T Barron, Ravi Ramamoorthi, and Ren Ng. Nerf: Representing scenes as neural radiance fields for view synthesis. *Communications of the ACM*, 65(1):99–106, 2021. 3
- [20] Nasir Mohammad Khalid, Tianhao Xie, Eugene Belilovsky, and Tiberiu Popa. Clip-mesh: Generating textured meshes from text using pretrained image-text models. In *SIGGRAPH Asia 2022 conference papers*, pages 1–8, 2022. 2, 3
- [21] Thomas Müller, Alex Evans, Christoph Schied, and Alexander Keller. Instant neural graphics primitives with a multiresolution hash encoding. *ACM Transactions on Graphics (ToG)*, 41(4):1–15, 2022. 3
- [22] Ben Poole, Ajay Jain, Jonathan T Barron, and Ben Mildenhall. Dreamfusion: Text-to-3d using 2d diffusion. *arXiv preprint arXiv:2209.14988*, 2022. 2, 3, 6, 7, 9
- [23] Alec Radford, Jong Wook Kim, Chris Hallacy, Aditya Ramesh, Gabriel Goh, Sandhini Agarwal, Girish Sastry, Amanda Askell, Pamela Mishkin, Jack Clark, et al. Learning transferable visual models from natural language supervision. In *International conference on machine learning*, pages 8748–8763. PMLR, 2021. 2, 6
- [24] Aditya Ramesh, Prafulla Dhariwal, Alex Nichol, Casey Chu, and Mark Chen. Hierarchical text-conditional image generation with clip latents. *arXiv preprint arXiv:2204.06125*, 2022. 2
- [25] Robin Rombach, Andreas Blattmann, Dominik Lorenz, Patrick Esser, and Björn Ommer. High-resolution image synthesis with latent diffusion models. In *Proceedings of the IEEE/CVF conference on computer vision and pattern recognition*, pages 10684–10695, 2022. 2, 3
- [26] Chitwan Saharia, William Chan, Saurabh Saxena, Lala Li, Jay Whang, Emily L Denton, Kamyar Ghasemipour, Raphael Gontijo Lopes, Burcu Karagol Ayan, Tim Salimans, et al. Photorealistic text-to-image diffusion models with deep language understanding. *Advances in Neural Information Processing Systems*, 35:36479–36494, 2022. 2, 3
- [27] Johannes L Schönberger, Enliang Zheng, Jan-Michael Frahm, and Marc Pollefeys. Pixelwise view selection for unstructured multi-view stereo. In *Computer Vision–ECCV 2016: 14th European Conference, Amsterdam, The Netherlands, October 11–14, 2016, Proceedings, Part III 14*, pages 501–518. Springer, 2016. 3
- [28] Christoph Schuhmann, Romain Beaumont, Richard Vencu, Cade Gordon, Ross Wightman, Mehdi Cherti, Theo Coombes, Aarush Katta, Clayton Mullis, Mitchell Wortsman, et al. Laion-5b: An open large-scale dataset for training next generation image-text models. *Advances in Neural Information Processing Systems*, 35:25278–25294, 2022. 3
- [29] Tianchang Shen, Jun Gao, Kangxue Yin, Ming-Yu Liu, and Sanja Fidler. Deep marching tetrahedra: a hybrid representation for high-resolution 3d shape synthesis. *Advances in Neural Information Processing Systems*, 34:6087–6101, 2021. 2
- [30] Jiaxiang Tang, Hang Zhou, Xiaokang Chen, Tianshu Hu, Er-rui Ding, Jingdong Wang, and Gang Zeng. Delicate textured mesh recovery from nerf via adaptive surface refinement. *arXiv preprint arXiv:2303.02091*, 2023. 3
- [31] Christina Tsalicoglou, Fabian Manhardt, Alessio Tonioni, Michael Niemeyer, and Federico Tombari. Textmesh: Generation of realistic 3d meshes from text prompts. *arXiv preprint arXiv:2304.12439*, 2023. 2, 3, 6, 7, 9
- [32] Fangjinhua Wang, Silvano Galliani, Christoph Vogel, Pablo Speciale, and Marc Pollefeys. Patchmatchnet: Learned multi-view patchmatch stereo. In *Proceedings of the IEEE/CVF conference on computer vision and pattern recognition*, pages 14194–14203, 2021. 3
- [33] Peng Wang, Lingjie Liu, Yuan Liu, Christian Theobalt, Taku Komura, and Wenping Wang. Neus: Learning neural implicit surfaces by volume rendering for multi-view reconstruction. *arXiv preprint arXiv:2106.10689*, 2021. 2, 3
- [34] Zhengyi Wang, Cheng Lu, Yikai Wang, Fan Bao, Chongxuan Li, Hang Su, and Jun Zhu. Prolificdreamer: High-fidelity and diverse text-to-3d generation with variational score distillation. *arXiv preprint arXiv:2305.16213*, 2023. 2, 3
- [35] Qingshan Xu and Wenbing Tao. Multi-scale geometric consistency guided multi-view stereo. In *Proceedings of the IEEE/CVF Conference on Computer Vision and Pattern Recognition*, pages 5483–5492, 2019. 3
- [36] Jiayu Yang, Jose M Alvarez, and Miaomiao Liu. Non-parametric depth distribution modelling based depth inference for multi-view stereo. In *Proceedings of the IEEE/CVF Conference on Computer Vision and Pattern Recognition*, pages 8626–8634, 2022. 3
- [37] Yao Yao, Zixin Luo, Shiwei Li, Tian Fang, and Long Quan. Mvsnet: Depth inference for unstructured multi-view stereo. In *Proceedings of the European conference on computer vision (ECCV)*, pages 767–783, 2018. 3
- [38] Yao Yao, Zixin Luo, Shiwei Li, Tianwei Shen, Tian Fang, and Long Quan. Recurrent mvsnet for high-resolution multi-view stereo depth inference. In *Proceedings of the IEEE/CVF conference on computer vision and pattern recognition*, pages 5525–5534, 2019. 3
- [39] Yao Yao, Zixin Luo, Shiwei Li, Jingyang Zhang, Yufan Ren, Lei Zhou, Tian Fang, and Long Quan. Blendedmvs: A large-scale dataset for generalized multi-view stereo networks. In *Proceedings of the IEEE/CVF conference on computer vision and pattern recognition*, pages 1790–1799, 2020. 3

- [40] Lior Yariv, Jiatao Gu, Yoni Kasten, and Yaron Lipman. Volume rendering of neural implicit surfaces. *Advances in Neural Information Processing Systems*, 34:4805–4815, 2021. 3, 4
- [41] Kai Zhang, Gernot Riegler, Noah Snaveley, and Vladlen Koltun. Nerf++: Analyzing and improving neural radiance fields. *arXiv preprint arXiv:2010.07492*, 2020. 3
- [42] Lvmin Zhang and Maneesh Agrawala. Adding conditional control to text-to-image diffusion models. *arXiv preprint arXiv:2302.05543*, 2023. 3
- [43] Enliang Zheng, Enrique Dunn, Vladimir Jojic, and Jan-Michael Frahm. Patchmatch based joint view selection and depthmap estimation. In *Proceedings of the IEEE Conference on Computer Vision and Pattern Recognition*, pages 1510–1517, 2014. 3